Chemical Science

RSC Publishing

EDGE ARTICLE

View Article Online
View Journal | View Issue

Cite this: *Chem. Sci.*, 2013, **4**, 4168

Therapeutic nanoworms: towards novel synthetic dendritic cells for immunotherapy†

Subhra Mandal,‡[a] Zaskia H. Eksteen-Akeroyd,‡[b] Monique J. Jacobs,[b] Roel Hammink,[b] Matthieu Koepf,§[b] Annechien J. A. Lambeck,¶[a] Jan C. M. van Hest,[c] Christopher J. Wilson,[b] Kerstin Blank,*[b] Carl G. Figdor*[a] and Alan E. Rowan*[b]

Received 20th May 2013
Accepted 30th July 2013

DOI: 10.1039/c3sc51399h

www.rsc.org/chemicalscience

A new class of antibody-functionalized, semi-flexible and filamentous polymers (diameter 5–10 nm, length ~200 nm) with a controlled persistence length, a high degree of stereoregularity and the potential for multiple simultaneous receptor interactions has been developed. We have decorated these highly controlled, semi-stiff polymers with T cell activating anti-CD3 antibodies and analyzed their application potential as simple synthetic mimics of dendritic cells (sDCs). Our sDCs do not only activate T cells at significantly lower concentrations than free antibodies or rigid sphere-like counterparts (PLGA particles) but also induce a more robust T cell response. Our novel design further yields sDCs that are biocompatible and non-toxic. The observed increased efficacy highlights the importance of architectural flexibility and multivalency for modulating T cell response and cellular function in general.

Introduction

The innate immune system is the body's first line of defence against invaders like pathogens and cancerous cells. Among the various cell types of the innate immune system, dendritic cells (DCs), also known as "professional" antigen-presenting cells (APCs) are of prime importance.[1] The knowledge about DCs has increased tremendously in the last 30 years[2] and their applicability for cancer immunotherapy has been investigated. *Ex vivo* generated DCs, when loaded with tumour lysates, tumour antigen-derived peptides or whole tumour proteins, have demonstrated enhanced anti-cancer immune responses.[3] Clinical studies have shown the potential of DCs as an autologous vaccine for cancer immunotherapy.[4,5] In spite of their potency, the application of *ex vivo* DCs is so far limited by their availability. Growth of *ex vivo* DCs is both labour and resource intensive. The requirement to generate a tailor made vaccine for every patient[6,7] means that *ex vivo* DCs are not economically sustainable. The aforementioned inefficiencies in the production of *ex vivo* DC's has inspired investigators to design artificial antigen-presenting cells (aAPCs) as alternatives.

Extensive studies on DC/T cell interactions *in vitro* have shown that the activation of T cells proceeds *via* a pre-clustering of MHC–peptide complexes in microdomains. These microdomains subsequently cluster into the so-called 'immune synapse' (IS).[8,9] Similar to many extracellular biological recognition processes, T cell activation consequently requires the simultaneous multivalent interaction of a number of receptors to initiate clustering. Molecular constructs that are able to mimic this simultaneous multivalent binding have a higher efficacy by increasing the avidity.[10–12] Further, activation does not only involve one type of receptor but instead multiple receptors that interact with different activation inducing molecules (*i.e.* MHC–peptides, co-stimulatory adhesion molecules, *etc.*).

The first generation of aAPCs, microbead-based DCs, have shown a marked advantage in expanding specific T cells under laboratory conditions compared to free MHC–peptide complexes. Their efficacy for long-term T cell expansion has been limited, however.[13] Unlike aAPCs, natural APCs have the ability to conform to the cell surface topography and allow the dynamic movement of receptor–ligand complexes to form the IS that ultimately causes T cell activation. Most likely the rigid sphere morphology of these microbead based aAPCs hinders the efficient formation of multivalent interactions with the

[a]*Department of Tumour Immunology, Nijmegen Centre for Molecular Life Sciences, Radboud University Nijmegen, Geert Grooteplein 26, 6525 GA Nijmegen, The Netherlands. E-mail: C.Figdor@ncmls.ru.nl*

[b]*Department of Molecular Materials, Institute for Molecules and Materials, Radboud University Nijmegen, 6525 AJ Nijmegen, The Netherlands. E-mail: k.blank@science.ru.nl; a.rowan@science.ru.nl*

[c]*Department of Bio-Organic Chemistry, Institute for Molecules and Materials, Radboud University Nijmegen, 6525 AJ Nijmegen, The Netherlands*

† Electronic supplementary information (ESI) available: Synthesis and characterization of the poly(isocyano peptide), of the αCD3–sDC bioconjugate and the αCD3–PLGA particles; experimental methods for the cell viability tests, the T cell activation tests as well as the confocal microscopy experiments. See DOI: 10.1039/c3sc51399h

‡ Authors contributed equally.

§ Present address: Energy Sciences Institute, Yale University, 300 Heffernan Drive, West Haven, CT 06516, USA.

¶ Present address: Department of Laboratory Medicine, Transplantation & Clinical Immunology, University Medical Center Groningen, University of Groningen, 9700 RB Groningen, The Netherlands.

T cells.[14,15] These aAPCs lack the plasma membrane fluidity of natural APCs that allows for the dynamic movement of these complexes to the IS site.[16] Soft spherical aAPCs, such as liposomes,[17] have overcome the membrane fluidity constraint enhancing T cell activation over and above that observed for the rigid sphere models, suggesting that the IS can form more efficiently if a dynamic movement of both binding partners can take place (Fig. 1).

Besides an efficient formation of the IS, also the number of receptor–ligand interactions involved in IS formation is known to play an important role in T cell activation. The number of interactions is dictated by the size and the morphology of the particle. In general, for rigid spherical particles the number of ligands available to participate in the required simultaneous interaction is limited by its topology.[17–19] Second-generation immunotherapeutic delivery vehicles have, therefore, explored extended aspect ratio topologies such as filamentous or rod-like particles. These extended aspect ratio structures have utilized either copolymer filomicelles[20] or decorated carbon nanotubes (CNTs).[21] Both filomicelles and CNTs have demonstrated a higher activity compared to their spherical counterparts.[21,22] This marked increase in efficacy is most likely a result of the larger surface-to-volume ratio that allows a more effective loading. If the micelle area is held constant for a given mass of co-polymer their effective loading is increased by 50% compared to the corresponding sphere.[20] Besides the increased effective loading that may aid in enhancing multivalent binding, filamentous or rod-like particles also show longer circulation times in the body that might play an additional advantageous role in T cell activation.[20]

The design criteria for an ideal synthetic dendritic cell (sDC) should incorporate the described knowledge gained from aAPCs and commonly used therapeutic delivery vehicles. It should combine the above characteristics of a high aspect ratio, a flexible architecture and multiple interactions to achieve highly efficient T cell activation. The sDCs should further possess an extended half-life and a low systemic toxicity.[23–25]

Here, we propose a fundamentally new design of sDCs that have the potential to fulfil all of the above criteria. Our strategy to building these novel delivery vehicles is based on a new class of rod-like, semi-stiff and water-soluble polymers derived from oligoethylene oxide substituted poly(isocyano peptides).[26,27] Poly(isocyano peptides) consist of a helical polyisocyanide backbone. This backbone carries peptide functionalized side chains that are attached to every carbon stabilizing the helix through hydrogen bonding.[28–30] These polymers can be up to 2 μm long and exhibit a well-defined stereoregularity[31] as well as a controlled stiffness that can be tuned between persistence lengths (L_P) of 5 nm to 200 nm.[26,32] Since in principle every individual monomer can be substituted with a functional unit, a versatile synthon for the design of multivalent filamentous sDCs is easily obtained (Fig. 2).

Our hypothesis is that such a semi-stiff poly(isocyano peptide) decorated with effector molecules rapidly docks on T cells (Fig. 2a and b). The semi-stiffness of the poly(isocyano peptide) will then allow all effector molecules on the sDC to bind to neighbouring receptors on the same cell (Fig. 2c). This is not possible for a rigid spherical bead or a flexible random-coil polymer, where multivalent interactions require entropically non-favourable, extended polymer conformations.[10,12] Subsequently, using a semi-stiff polymer, these receptor sites will be able to cluster with a concomitant contraction of the polymer backbone to form the IS while retaining the activated state (Fig. 2d). To test our design strategy, we functionalized these sDCs with anti-CD3 antibodies (αCD3–sDC), that are known to cause T cell activation, and compared their efficacy with microbead based aAPCs (αCD3–PLGA) and free αCD3 antibodies.

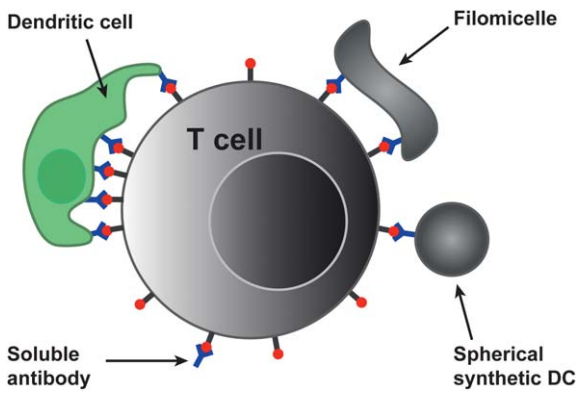

Fig. 1 Schematic diagram illustrating different systems for T cell activation.

Results and discussion

Synthesis and characterization of the αCD3–sDCs

Synthetic dendritic cells (sDCs) carrying T cell stimulating αCD3 antibodies have been synthesized from semi-stiff poly(isocyano peptides). To obtain these sDCs, an azide containing poly(isocyano peptide) was synthesized in the first step (see ESI† for synthetic procedures). This was achieved by co-polymerizing a mixture of an azide-functionalized monomer and a methoxy-functionalized monomer using a 1 : 100 molar ratio resulting in a random copolymer (Scheme 1).

The obtained polymers have a degree of polymerization DP = 1633 and a length between 150 nm and 200 nm (Table S1†). The statistical spacing between azide groups is 10 nm. These azide groups were subsequently used to couple BCN-functionalized streptavidin (SAv) to the polymer backbone using a strain-promoted azide alkyne click (SPAAC) reaction.[33] The obtained SAv-functionalized polymer contains on average one SAv molecule every 40–50 nm (Fig. 3), as determined with AFM. sDCs were obtained by adding biotinylated αCD3 antibodies yielding αCD3–sDC. When preparing the αCD3–sDC, the ratio of αCD3 to SAv on the polymer was adjusted such that on average every SAv was bound to one αCD3 antibody (Fig. S6†). Consequently, an average polymer with a length of 150–200 nm contains between 3 and 5 αCD3 antibodies.

Cell viability measurements

Before testing the efficacy of these novel sDCs on peripheral blood lymphocytes (PBLs), cell viability studies were carried out

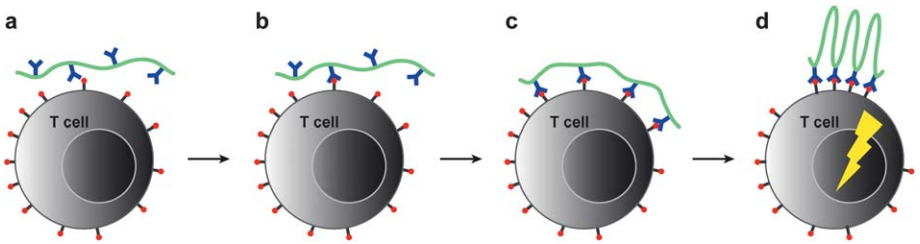

Fig. 2 Stages of sDC binding and T cell activation. (a) The mobility of the sDC assists in locating the T cell; (b) sDC docks onto the T cell; (c) attachment to multiple recognition sites; (d) sDC contracting/clustering at the recognition sites, IS formation.

to study their biocompatibility. PBLs exposed to αCD3–sDC or free αCD3 at different concentrations exhibited no significant decrease in cell viability (MTT assay; Fig. 4a). At higher αCD3 concentrations even an increase in the number of cells was observed, which can be explained by induction of T cell proliferation by the αCD3 antibodies (*vide infra*). Even after prolonged incubation times, cell viability remained constant between 90 and 100% even up to 72 hours (Trypan Blue assay; Fig. 4b).

T cell activation

In subsequent experiments, the capacity of αCD3–sDC to activate T cells was determined in comparison to free αCD3 antibodies, streptavidin bound αCD3 (αCD3–SAv) and the corresponding isotype control (mIgG2a–sDC). After clustering of CD3 on the T cells, intracellular signalling results in direct activation as demonstrated by expression of the early T cell activation marker CD69.[34] Activated T cells further show enhanced secretion of IFNγ as a late activation event[35] and eventual T cell proliferation is observed.[36]

At saturating concentrations (>50 ng mL^{-1}), CD69 expression was at its maximum, for both the αCD3–sDC and the controls including free αCD3 and αCD3–SAv (Fig. 5a). At low concentrations (1–20 ng mL^{-1}), however, the αCD3–sDCs were ~2.5 fold more effective in inducing T cell activation when compared to the αCD3 and αCD3–SAv controls. Similarly, the

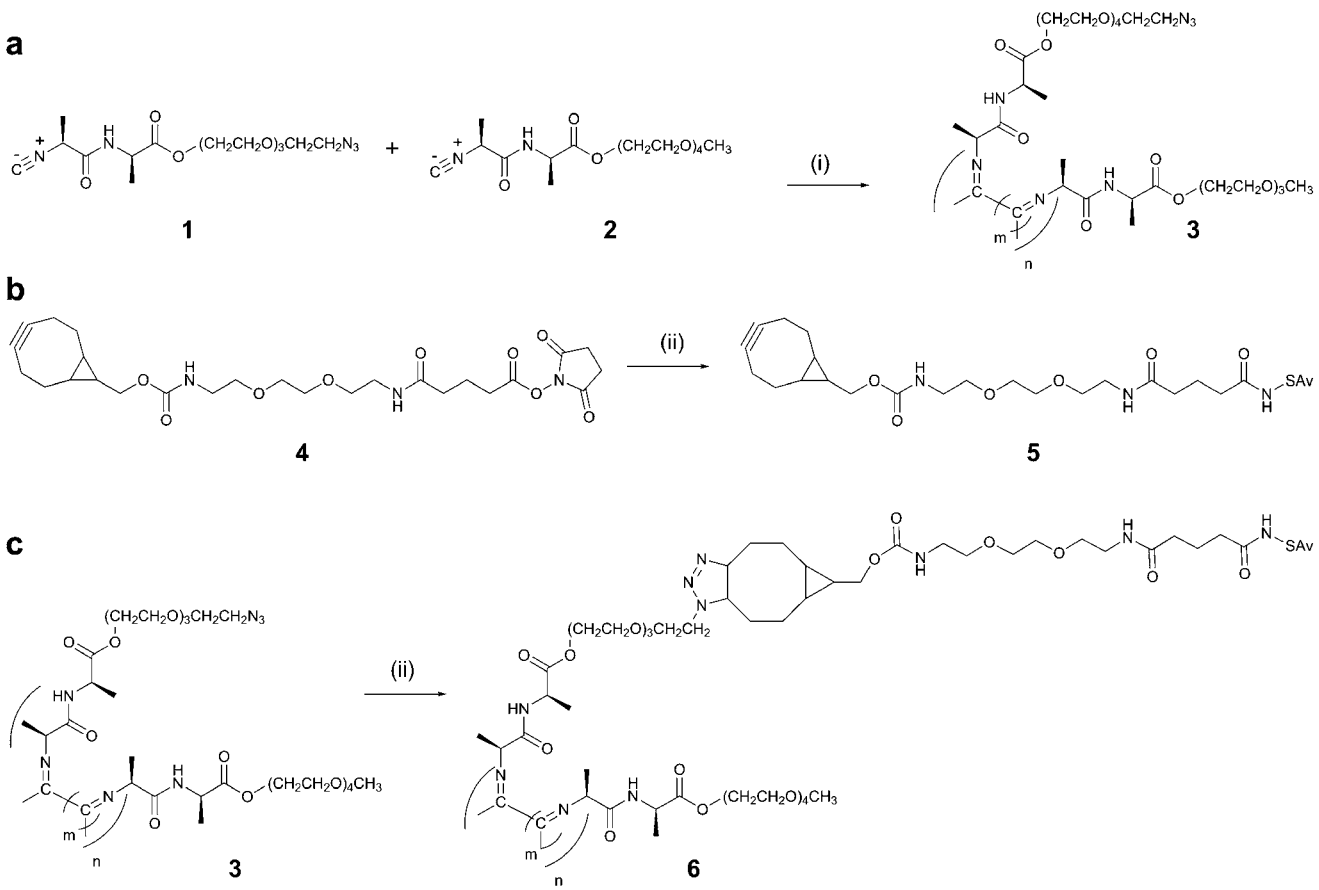

Scheme 1 Synthetic scheme to obtain streptavidin (SAv) functionalized poly(isocyano peptides). (a) Random co-polymerization of the azide (**1**) and the methoxy (**2**) monomers to obtain the azide-functionalized polymer (**3**), (i) $Ni(Cl_2O_4)_2 \cdot 6H_2O$, toluene; (b) coupling of BCN–NHS (**4**) to SAv, (ii) 4 days at 4 °C in 10 mM borate buffer pH 8.5; (c) synthesis of the SAv–polymer bioconjugate (**6**).

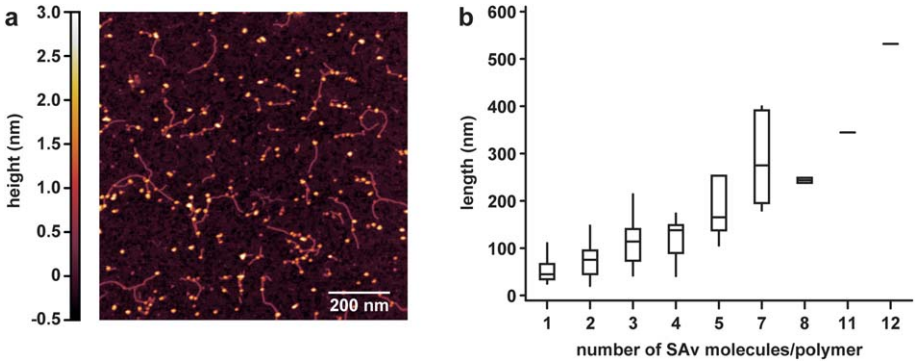

Fig. 3 AFM analysis of polymer **6**. (a) Representative AFM image clearly showing the SAv molecules (bright dots) attached to the polymer; (b) number of SAv molecules per polymer.

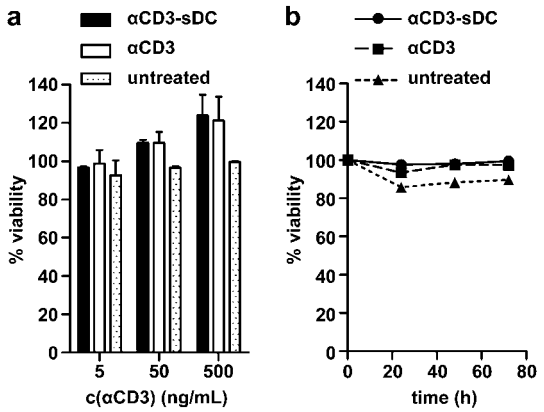

Fig. 4 Viability of PBLs exposed to αCD3–sDC. (a) MTT assay showing cell viability as a function of αCD3 concentration (incubation time 24 h). (b) Trypan Blue assay showing cell viability as a function of incubation time (αCD3 concentration of 200 ng mL^{-1} for both αCD3–sDC and free αCD3). The results represent the mean ± s.e.m. ($n = 3$).

αCD3–sDC activated T cells released 2–3 fold higher amounts of IFNγ than the tested controls (Fig. 5b). Taken together, these findings and the additional controls shown in Fig. S7† indicate that αCD3–sDC induces a more robust T cell activation when compared to T cells exposed to free αCD3 or αCD3–SAv.

To substantiate the above findings, T cell activation was followed over time at a low effective treatment concentration (5 ng mL^{-1} αCD3 for both αCD3–sDC and free αCD3). The αCD3–sDC treated T cells were activated at significantly earlier time points (Fig. 5c). Over prolonged exposure, T cell activation increased up to ~35%. In comparison, T cell activation following treatment with free αCD3 shows a delay in T cell activation (10 hours *vs.* 7 hours for αCD3–sDC) and a lower percentage of activated T cells (only ~10–15%). Finally, the ability of αCD3–sDC to induce T cell proliferation was tested (50 ng mL^{-1} αCD3 for both αCD3–sDC and free αCD3). In line with the above results, a 2–3 fold higher number of proliferated T cells was detected when the T cells were treated with αCD3–sDC (Fig. 5d). Treatment with αCD3–sDC leads to a constant increase in the proliferation rate until 72 h of treatment. The observed decrease in the number of T cells at 96 h is likely resulting from nutrient depletion in the growth medium at high cell concentrations.

To investigate the importance of the structural architecture of our novel sDCs, their efficacy was compared to spherical αCD3–PLGA particles (1.8 μm diameter, see ESI†). The worm-like αCD3–sDCs were ~7 fold more efficient in stimulating T cell activation (CD69 expression) when compared to αCD3–PLGA particles, even at concentrations as low as 1 ng mL^{-1} (Fig. 6a). Also the production of IFNγ was ~3 fold higher when compared to αCD3–PLGA particles (Fig. 6b). Together these observations indicate that our αCD3–sDCs do not only activate T cells significantly better at lower concentrations. They also induce the highest IFNγ production when compared with solid particle based DCs.

This difference in efficacy cannot be explained with the number of receptor–ligand interactions that can form when using αCD3–sDCs (~3–5 interactions) or αCD3–PLGA particles (~1–10 interactions; see ESI†). This similar number of possible interactions for both geometries clearly suggests that it is not the density of αCD3 but the ability of polymer-based sDCs to flexibly adjust to the spacing of receptors and to dynamically form the immune synapse that leads to the superior activity of our sDCs. In other words, multiple static interactions are not sufficient. It has been postulated that a more dynamic anisotropic interaction between the binding partners is required to induce and enhance T cell activation.[37,38] Unlike the static shape of the hard sphere model, the controlled stiffness of the αCD3–sDC filament has the capacity to 'concertina' in response to the receptor clustering events associated with the formation of the immune synapse (Fig. 2).

Localization of αCD3–sDC on the cell surface

To investigate the molecular process in more detail and to understand how the sDCs interact with T cells, binding studies were performed with fluorescently labelled αCD3–sDCs. The PBLs were incubated with different concentrations of either fluorescein labelled αCD3–sDCs (FαCD3–sDC) or free αCD3 (FαCD3) for 24 hours (see ESI†). Subsequently, the number of fluorescent cells was determined using a laser scanning confocal microscope (Fig. 7 and S9†).

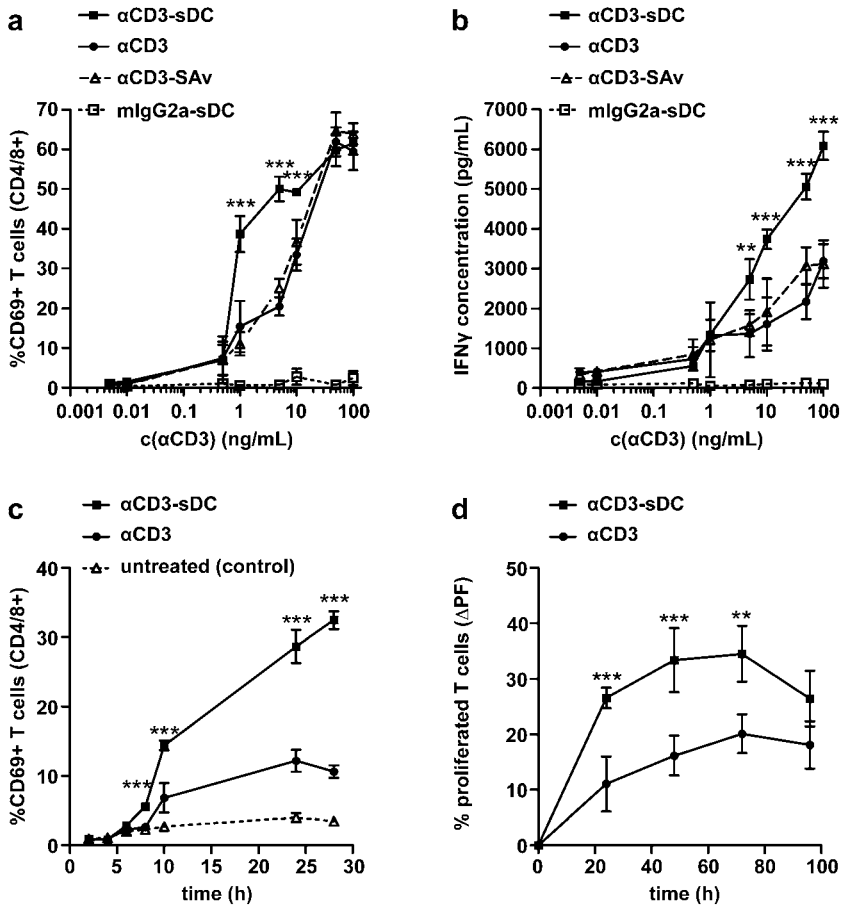

Fig. 5 T cell activation profile upon treatment at different concentrations and after different time points. (a) Percentage of T cells showing CD69 expression and (b) IFNγ release at different αCD3 concentrations (incubation time 24 h); (c) percentage of T cells showing CD69 expression after different incubation times (αCD3 concentration 5 ng mL^{-1}); (d) T cell proliferation estimated using a CFSE assay (αCD3 concentration 50 ng mL^{-1}). The values were normalized against the untreated control. Each value represents the mean ± s.e.m. ($n = 4$). The asterisks (*) indicate the statistical significance (*, **, *** $p \leq 0.05$, 0.01, 0.001) of αCD3–sDC compared to αCD3.

At high concentrations (50 and 100 ng mL^{-1}) the relative number of T cells that show binding of FαCD3–sDC on their surface was comparable to the percentage of cells that have been treated with free FαCD3. In the low concentration range (≤20 ng mL^{-1}), however, a higher fraction of PBLs carrying FαCD3–sDC was observed when compared to the cells treated with free FαCD3. This result clearly explains the higher efficacy of the αCD3–sDCs in the low concentration range (Fig. 7a).

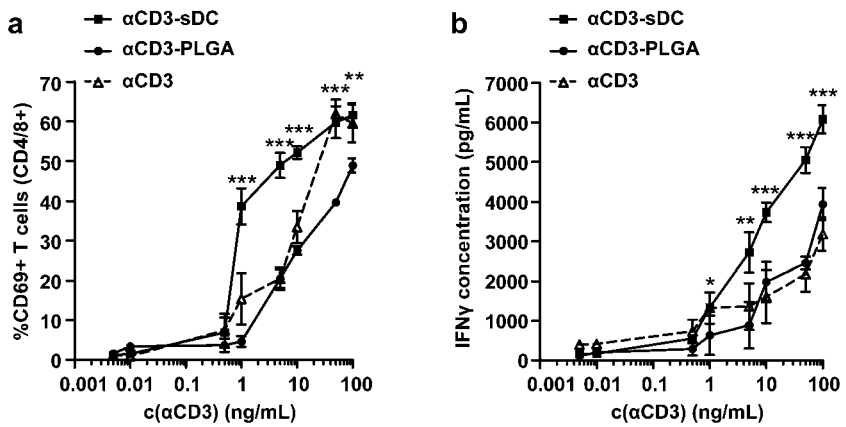

Fig. 6 Comparison of αCD3–sDC with spherical αCD3–PLGA. (a) Percentage of T cells showing CD69 expression and (b) IFNγ release at different αCD3 concentrations (incubation time 24 h); the results represent the mean ± s.e.m. ($n = 3$). The asterisks (*, **, ***$p = <0.05$, 0.01, 0.001) indicate the statistical significance of αCD3–sDC compared to αCD3.

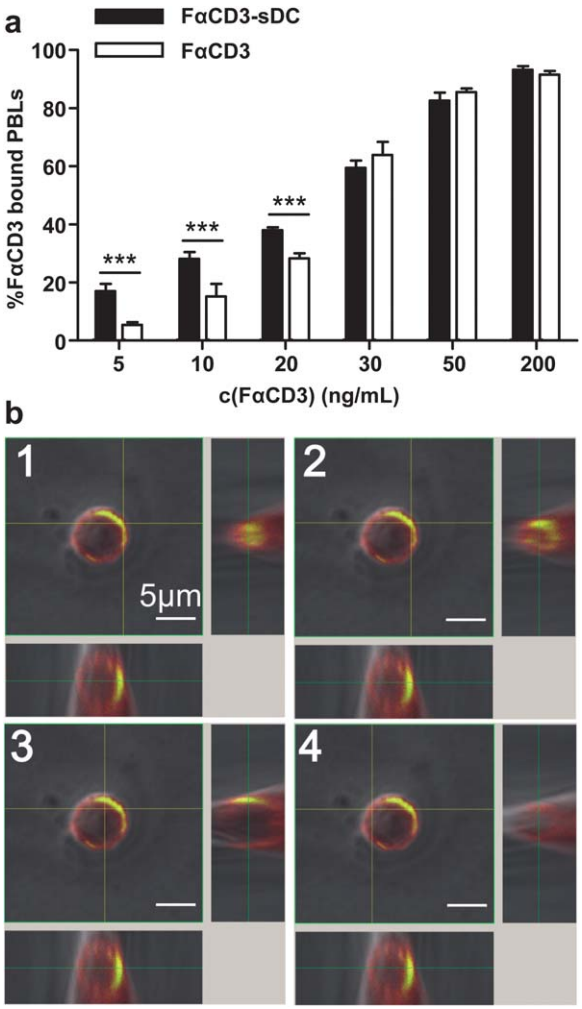

Fig. 7 αCD3–sDC binding and location on the cell. (a) percentage of PBLs showing bound FαCD3 or FαCD3–sDC after 24 hours of treatment. The result shows the mean ± s.e.m. ($n = 3$). The significance of αCD3–sDC compared to αCD3 is indicated by the asterisks (***$p \leq 0.001$). (b) Orthographic projection of one PBL illustrating αCD3–sDC clustering/binding (yellow; co-localization of red and green fluorescence). The fluorescence image is merged with a DIC image. The series shows optical cross sections over the *y*-coordinate (*x*- and *z*-coordinate constant), demonstrating the αCD3–sDC distribution on the cell.

Besides more efficient binding, 3D images taken after 24 hours further reveal that FαCD3–sDC remained co-localized on the membrane indicating that no receptor internalization has been taking place (Fig. 7b).

Summarizing the above results, this new class of semi-stiff and filamentous polymers serves as an ideal scaffold for functionalization with antibodies to allow for multiple, simultaneous receptor interactions. These novel sDCs do not only activate T cells at significantly lower concentrations than free antibodies and their rigid sphere-like PLGA counterparts but also induce a faster T cell response. Docking of the first antibody to the T cell increases the effective molarity of αCD3 at the cell surface thereby increasing the probability for the remaining antibodies to bind (Fig. 2b). It is known that T cell stimulation by αCD3 in solution causes internalization of the CD3 leading to termination of the T cell response.[39] The experiments with fluorescently labelled FαCD3–sDC have indicated that FαCD3–sDC remains bound on the T cell surface even after 24 h of treatment. The semi-stiff, filamentous morphology of the αCD3–sDCs consequently does not only lead to a significantly higher and earlier (CD69 expression) but also to a more sustained T cell response compared to the free antibody and the spherical geometry. This result is supported by the expression of the late stage activation marker INFγ and the associated higher T cell proliferation rates. These findings have important consequences for the therapeutic use of αCD3 antibodies, which show *in vivo* toxicity at high concentrations.[40] As our αCD3–sDCs show T cell activation at lower concentrations compared to free αCD3 antibodies, this new design can help to overcome these toxicity problems and widen the therapeutic window of αCD3 antibodies.

Despite their clearly proven potential as a DC mimic, a number of open questions remain. The stiffness of the polymer combined with the density of effector molecules appears to be the crucial parameter for efficient T cell activation. Antibody-functionalized poly(isocyano peptides) are an ideal scaffold to investigate the importance of these parameters in a systematic way. Both the density of effector molecules as well as the polymer stiffness can be easily tuned for this new class of functional polymers. Experiments are currently underway to study the role of the polymer length, the polymer stiffness and the effector molecule loading on T cell activation.

Conclusions

In this report we demonstrate that multivalency in combination with a controlled semi-stiffness are key parameters for designing potentially therapeutically active vehicles that closely mimic natural DCs. Using our novel sDC design, we observe a more efficient as well as more sustained T cell response. This enhanced activity clearly validates the final stage of the proposed binding mechanism (Fig. 2d) that requires the sDC to respond to the processes occurring on the T cell surface during formation of the immune synapse. Having shown the potency of our sDCs, our next goal is a more detailed investigation of the sDC induced T cell activation mechanism. This will ultimately allow us to increase their efficacy even further. To develop the presented sDC system for clinical applications against cancer, the αCD3 antibodies will be replaced with MHC–peptide complexes and co-stimulatory molecules, necessary for highly efficient T cell activation. Cytokines can be coupled in addition to further shape the T cell response. Ultimately, after characterization of their *in vivo* behaviour, our sDCs have the potential to become a highly efficient and cost-effective nanovaccine for cancer immunotherapy. Besides cancer immunotherapy, the semi-stiff poly(isocyano peptides) scaffold might be used for other applications where multivalent binding is essential. Multivalency, for example, plays an important role in drug targeting. Functionalization of the scaffold with effector molecules as well as targeting and imaging moieties can potentially lead to a more efficient accumulation and detection of the therapeutic agent at the desired site of action opening up a far bigger range of possible therapeutic and diagnostic applications.

Acknowledgements

This work was supported by grants from the Dutch Cancer Society (grants KUN2006-3699 and KUN2009-4402), the Dutch government to the Netherlands Institute for Regenerative Medicine (NIRM, grant FES0908), the European Research Council (ERC; grant ERC-2010-AdG269019, C.G.F.), the Netherlands Organization for Scientific Research (NWO; Spinoza award 2006, C.G.F; VICI grant 700.56.444, A.E.R.; VIDI grant 700.58.430, K.B.), the Foundation for Fundamental Research on Matter (FOM; grant 10PR2791) as well as NanoNext (grants 7A.06 and 3D.12).

References

1 J. Banchereau and R. M. Steinman, *Nature*, 1998, **392**, 245–252.
2 R. M. Steinman and Z. A. Cohn, *J. Exp. Med.*, 1973, **137**, 1142–1162.
3 L. Fong and E. G. Engleman, *Annu. Rev. Immunol.*, 2000, **18**, 245–273.
4 A. Ballestrero, D. Boy, E. Moran, G. Cirmena, P. Brossart and A. Nencioni, *Adv. Drug Delivery Rev.*, 2008, **60**, 173–183.
5 I. Houtenbos, T. M. Westers, G. J. Ossenkoppele and A. A. van de Loosdrecht, *Immunobiology*, 2006, **211**, 677–685.
6 M. Oelke, C. Krueger, R. L. Giuntoli and J. P. Schneck, *Trends Mol. Med.*, 2005, **11**, 412–420.
7 W. Gong, M. Ji, Z. Cao, L. Wang, Y. Qian, M. Hu, L. Qian and X. Pan, *Cell. Mol. Immunol.*, 2008, **5**, 47–53.
8 F. Giannoni, J. Barnett, K. Bi, R. Samodal, P. Lanza, P. Marchese, R. Billetta, R. Vita, M. R. Klein, B. Prakken, W. W. Kwok, E. Sercarz, A. Altman and S. Alban, *J. Immunol.*, 2005, **174**, 3204–3211.
9 M. L. Dustin, *Immunity*, 2004, **21**, 305–314.
10 S. Liu and K. L. Kiick, *Macromolecules*, 2008, **41**, 764–772.
11 S. Liu, R. Maheshwari and K. L. Kiick, *Macromolecules*, 2009, **42**, 3–13.
12 C. Fasting, C. A. Schalley, M. Weber, O. Seitz, S. Hecht, B. Koksch, J. Dernedde, C. Graf, E. W. Knapp and R. Haag, *Angew. Chem., Int. Ed.*, 2012, **51**, 10472–10498.
13 I. Laux, A. Khoshnan, C. Tindell, D. Bae, X. Zhu, C. H. June, R. B. Effros and A. Nel, *Clin. Immunol.*, 2000, **96**, 187–197.
14 H. A. Anderson, E. M. Hiltbold and P. A. Roche, *Nat. Immunol.*, 2000, **1**, 156–162.
15 A. B. Vogt, S. Spindeldreher and H. Kropshofer, *Immunol. Rev.*, 2002, **189**, 136–151.
16 B. Prakken, M. Wauben, D. Genini, R. Samodal, J. Barnett, A. Mendivil, L. Leoni and S. Albani, *Nat. Med.*, 2000, **6**, 1406–1410.
17 R. Zappasodi, M. Di Nicola, C. Carlo-Stella, R. Mortarini, A. Molla, C. Vegetti, S. Albani, A. Anichini and A. M. Gianni, *Haematologica*, 2008, **93**, 1523–1534.
18 E. Koffeman, E. Keogh, M. Klein, B. Prakken and S. Albani, *Methods Mol. Med.*, 2007, **136**, 69–86.
19 C. Schütz, M. Oelke, J. P. Schneck, A. Mackensen and M. Fleck, *Immunotherapy*, 2010, **2**, 539–550.
20 S. Cai, K. Vijayan, D. Cheng, E. M. Lima and D. E. Discher, *Pharm. Res.*, 2007, **24**, 2099–2109.
21 T. R. Fadel, E. R. Steenblock, E. Stern, N. Li, X. Wang, G. L. Haller, L. D. Pfefferle and T. M. Fahmy, *Nano Lett.*, 2008, **8**, 2070–2076.
22 Y. Geng, P. Dalhaimer, S. Cai, R. Tsai, M. Tewari, T. Minko and D. E. Discher, *Nat. Nanotechnol.*, 2007, **2**, 249–255.
23 E. Heister, V. Neves, C. Tîlmaciu, K. Lipert, V. S. Beltra, H. M. Coley, S. R. P. Silva and J. McFadden, *Carbon*, 2009, **47**, 2152–2160.
24 K. Rajagopal, D. A. Christian, T. Harada, A. Tian and D. E. Discher, *Int. J. Polym. Sci.*, 2010, 379286.
25 V. V. Shuvaev, M. A. Ilies, E. Simone, S. Zaitsev, Y. Kim, S. Cai, A. Mahmud, T. Dziubla, S. Muro, D. E. Discher and V. R. Muzykantov, *ACS Nano*, 2011, **5**, 6991–6999.
26 P. H. J. Kouwer, M. Koepf, V. A. A. Le Sage, M. Jaspers, A. M. van Buul, Z. H. Eksteen-Akeroyd, T. Woltinge, E. Schwartz, H. J. Kitto, R. Hoogenboom, S. J. Picken, R. J. M. Nolte, E. Mendes and A. E. Rowan, *Nature*, 2013, **493**, 651–655.
27 M. Koepf, H. J. Kitto, E. Schwartz, P. H. J. Kouwer, R. J. M. Nolte and A. E. Rowan, *Eur. Polym. J.*, 2013, **49**, 1510.
28 H. G. J. Visser, R. J. M. Nolte and W. Drenth, *Macromolecules*, 1985, **18**, 1818–1825.
29 J. M. van der Eijk, R. J. M. Nolte, W. Drenth and A. M. F. Hezemans, *Macromolecules*, 1980, **13**, 1391–1397.
30 J. J. Cornelissen, J. J. Donners, R. de Gelder, W. S. Graswinckel, G. A. Metselaar, A. E. Rowan, N. A. Sommerdijk and R. J. M. Nolte, *Science*, 2001, **293**, 676–680.
31 Z. Q. Wu, K. Nagai, M. Banno, K. Okoshi, K. Onitsuka and E. Yashima, *J. Am. Chem. Soc.*, 2009, **131**, 6708–6718.
32 A. M. van Buul, E. Schwartz, P. Brocorens, M. Koepf, D. Beljonne, J. C. Maan, P. C. M. Christianen, P. H. J. Kouwer, R. J. M. Nolte, H. Engelkamp, K. Blank and A. E. Rowan, *Chem. Sci.*, 2013, **4**, 2357–2363.
33 J. Dommerholt, S. Schmidt, R. Temming, L. J. A. Hendriks, F. P. J. T. Rutjes, J. C. M. van Hest, D. J. Lefeber, P. Friedl and F. L. van Delft, *Angew. Chem., Int. Ed.*, 2010, **49**, 9422–9425.
34 I. Yamashita, T. Nagata, T. Tada and T. Nakayama, *Int. Immunol.*, 1993, **5**, 1139–1150.
35 M. Murphy, R. Loudon, M. Kobayashi and G. Trinchieri, *J. Exp. Med.*, 1986, **164**, 263–279.
36 J. E. Kay, *Immunol. Lett.*, 1991, **29**, 51–54.
37 E. D. Zanders, J. R. Lamb, M. Feldmann, N. Green and P. C. L. Beverley, *Nature*, 1983, **303**, 625–627.
38 S. C. Balmert and S. R. Little, *Adv. Mater.*, 2012, **24**, 3757–3778.
39 C. Calabia-Linares, J. Robles-Valero, H. de la Fuente, M. Perez-Martinez, N. Martin-Cofreces, M. Alfonso-Perez, C. Gutierrez-Vazquez, M. Mittelbrunn, S. Ibiza, F. R. Urbano-Olmos, C. Aguado-Ballano, C. O. Sanchez-Sorzano, F. Sanchez-Madrid and E. Veiga, *J. Cell Sci.*, 2011, **124**, 820–830.
40 J. D. Ellenhorn, R. Hirsch, H. Schreiber and J. A. Bluestone, *Science*, 1988, **242**, 569–571.

